Comparison of clustering effects in ^{12}C fragmentation among $p+^{12}$C, $\alpha+^{12}$C, and ^{14}N$+^{12}$C reactions: Excitation of α-cluster degrees of freedom in nuclear collisions

Hiroki Takemoto and Hisashi Horiuchi
Department of Physics, Kyoto University, Kyoto 606-01, Japan

Akira Ono
Department of Physics, Tohoku University, Sendai 980-77, Japan

(Received 5 September 1997)

We examine ^{12}C fragmentation in $p+^{12}$C, $\alpha+^{12}$C, and ^{14}N$+^{12}$C reactions using antisymmetrized molecular dynamics. We compare ^{12}C fragmentation among the above three kinds of reactions and find that the alpha-clustering effect in ^{12}C fragmentation depends on the projectile and also on the incident energy. In proton induced reactions ^{4}He fragments are scarcely produced at the early stage of the reaction in a wide range of incident energy. On the other hand, in α and ^{14}N induced reactions many ^{4}He fragments are produced during the dynamical stage at a lower incident energy but fewer ^{4}He fragments are produced with increasing incident energy. We indicate that this abundance of ^{4}He fragments at a lower incident energy in α and ^{14}N induced reactions is due to the excitation of ^{12}C to states with an excitation energy of 7–15 MeV which have the alpha-cluster structure. We see that the upper limit of the incident energy which gives rise to the dynamical production of ^{4}He fragments is lower in the α induced reaction than in the ^{14}N induced reaction. We show that the excitation to the clustering states is caused by the mean field from the projectile and that nucleon-nucleon collisions work to destroy this excitation. We will see that the disappearance of the excitation to the clustering states at high incident energies is partly due to the weakened effect of the mean field of the projectile and partly due to the strengthened effect of nucleon-nucleon collision processes. [S0556-2813(98)04702-5]

PACS number(s): 25.70.Mn, 02.70.Ns, 21.60.Gx, 24.10.Cn

I. INTRODUCTION

In heavy ion reactions, there are or there are expected to be various kinds of mechanisms producing fragments, like coalescence, the participant-spectator mechanism, neck fragmentation, bubble fragmentation, the liquid-vapor phase transition, and so on [1]. Except for these mechanisms, we can consider the mechanism reflecting the nuclear structure. Especially, in this paper we focus on the fragmentation mechanism reflecting the alpha-cluster structure.

In general, self-conjugate $4n$ nuclei have anomalous excited states with an excitation energy of 7–15 MeV, which are recognized to be generated by the change of the structure from a shell-model-like one to a cluster one due to the activation of the clustering degrees of freedom [2]. In the ^{12}C case these anomalous levels including 0_2^+ at 7.65 MeV and 2_2^+ at 10.3 MeV have been recognized to have the 3α structure. Since the excitation energies of these levels are usually near or above the threshold of the breakup into constituent clusters, it is natural that the clustering effect is expected to play an important role in heavy ion reactions.

Microscopic simulation studies, such as Boltzmann-Uehling-Uhlenbeck (BUU), Vlasoz-Uehling-Uhlenbeck (VUU) [3] and quantum molecular dynamics (QMD) [4] studies, are very useful for investigating various kinds of reaction mechanisms systematically. But only a few theoretical studies of the mechanism reflecting the nuclear structure exist because most current simulation theories are of a semiclassical character and cannot describe quantum mechanical features such as the shell effect in heavy ion reactions. Antisymmetrized molecular dynamics (AMD) can describe the quantum character and the clustering degrees of freedom, since it treats the time development of the system wave function [5–7]. Hence by using AMD we can study the fragmentation related to the nuclear structure, especially the cluster structure in addition to many other mechanisms cited above. Many experimental studies related to such a mechanism have been reported, for example, the breakup of ^{16}O into 4α in the collisions of 25 MeV/nucleon ^{16}O with ^{159}Tb by Charity *et al.* [8], in the collisions of 32.5 MeV/nucleon ^{16}O with ^{197}Au by Harmon *et al.* [9], the breakup of ^{20}Ne in the collisions of 40 MeV/nucleon ^{20}Ne with ^{197}Au and ^{120}Sn by Charity *et al.* [10], the breakup of ^{24}Mg in the collisions of 25 and 35 MeV/nucleon ^{24}Mg with ^{197}Au by Samri *et al.* [11], and so on.

Recently we investigated the difference between ^{12}C and ^{14}N fragmentation in the ^{14}N$+^{12}$C reaction at 35 MeV/nucleon [12]. Since ^{12}C and ^{14}N have almost the same mass number, if the fragmentation from each nucleus is different, it indicates the existence of the fragmentation mechanism related to the nuclear structure. The calculated results were as follows.

(1) ^{4}He fragments from ^{12}C are more numerous than those from ^{14}N. This abundance from ^{12}C mainly originates from the dynamical process, while ^{4}He fragments from ^{14}N do not originate from the dynamical process but from the statistical decay process.

(2) The energy spectrum of ^{4}He fragments from ^{12}C, which are produced in the dynamical process, has the peak near the incident energy.

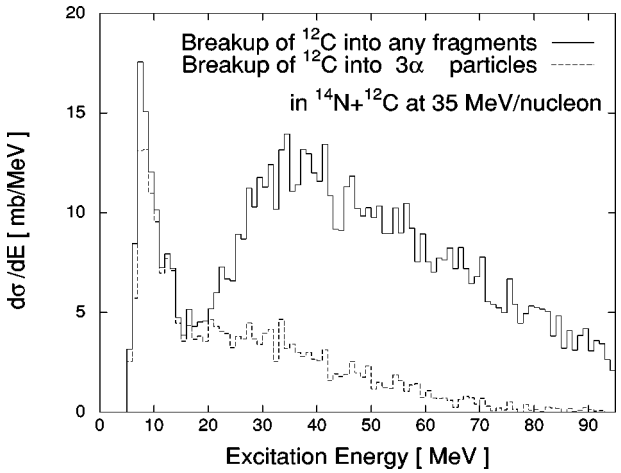

FIG. 1. Excitation energy spectra of ^{12}C just before its breakup during the dynamical process in ^{14}N+^{12}C at 35 MeV/nucleon. The way to calculate the excitation energy of isolated ^{12}C is explained in Sec. V. Solid and dashed lines indicate those just before the breakup of ^{12}C into any fragments and 3α particles, respectively.

(3) ^{4}He fragments from ^{12}C are produced most frequently through semi-peripheral collisions during the dynamical process.

(4) ^{12}C breaks up into 3α particles with the largest probability among all production events of ^{4}He fragments in the dynamical process.

From the study of the excitation energy spectra of ^{12}C before its breakup during the dynamical process, we concluded that the above features of ^{12}C fragmentation originate from the activation of alpha-cluster degrees of freedom. The excitation energy spectrum of ^{12}C before its breakup into *any fragments* during the dynamical process consists of two components, as is indicated by the solid line in Fig. 1. One distributes in the range 7–15 MeV and the other in the range above 15 MeV. Most of the events of the former component are such events that ^{12}C breaks up into *3α particles* during the dynamical process, as indicated by the dashed line in Fig. 1, and hence these excitation energies, 7–15 MeV, just correspond to the excited levels of ^{12}C which have the 3α-cluster structure. Accordingly the features mentioned above are due to the excitation of ^{12}C to the states which have the cluster structure.

In this paper we analyze $p+^{12}$C reactions at 26, 55, and 100 MeV, $\alpha+^{12}$C ones at 22.5 and 35 MeV/nucleon, and ^{14}N+^{12}C ones at 35 and 55 MeV/nucleon using antisymmetrized molecular dynamics. By comparing ^{12}C fragmentation in three kinds of reactions, we investigate the projectile-mass and incident-energy dependence of the alpha-clustering effect in ^{12}C fragmentation. From these investigations we make clear the effects of the mean field and nucleon-nucleon collision processes on the excitation of alpha-cluster degrees of freedom.

In the next section, we describe the AMD formalism briefly. A comparison of the AMD results with the experimental data is given in Sec. III, and the incident-energy dependence of ^{12}C fragmentation in ^{14}N, alpha, and proton induced reactions is discussed in Sec. IV. Section V gives the excitation energy spectra of ^{12}C before its breakup during the dynamical process and the evidence of the excitation of alpha-cluster degrees of freedom. In Sec. VI we show that the excitation of ^{12}C to its clustering excited states is caused by the mean field of the projectile and that nucleon-nucleon collisions work to destroy this excitation. Section VII gives a discussion of the ^{4}He-multiplicity channel. In Sec. VIII we discuss the excitation of ^{12}C compound states by showing the excitation energy spectra of ^{12}C at the end of the dynamical process. In Sec. IX we give a summary and conclusions.

II. BRIEF EXPLANATION OF AMD FORMALISM

The formalism of AMD was described in detail in Ref. [5], and only the outline of AMD is explained below. In AMD, the wave function of the A-nucleon system $|\Phi\rangle$ is described by a Slater determinant

$$|\Phi\rangle=\frac{1}{\sqrt{A!}}\det[\varphi_i(j)], \tag{1}$$

where

$$\varphi_i=\phi_{\mathbf{Z}_i}\chi_{\alpha_i}(\alpha_i=p\uparrow,p\downarrow,n\uparrow,n\downarrow) \tag{2}$$

and

$$\phi_{\mathbf{Z}_i}=\left(\frac{2\nu}{\pi}\right)^{3/4}\exp\left[-\nu\left(\mathbf{r}-\frac{\mathbf{Z}_i}{\sqrt{\nu}}\right)^2+\frac{1}{2}\mathbf{Z}_i^2\right]. \tag{3}$$

χ_{α_i} and $\phi_{\mathbf{Z}_i}$ represent the spin-isospin wave function and the spatial wave function of the ith single-particle state, respectively. ν is the width parameter which is independent of time and in the following calculations $\nu=0.16$ fm^{-2}. $Z=\{\mathbf{Z}_i\}$ represent the positions of the centers of Gaussians and, therefore, the A-body wave function $|\Phi\rangle$ is parametrized by Z. The time development of Z is determined by the time-dependent variational principle which leads to the following equation of motion for Z:

$$i\hbar\sum_{j\tau}C_{i\sigma j\tau}\frac{d}{dt}Z_{j\tau}=\frac{\partial\mathcal{H}}{\partial Z_{i\sigma}^*}\quad\text{and c.c.}, \tag{4}$$

$$C_{i\sigma j\tau}=\frac{\partial^2}{\partial Z_{i\sigma}^*\partial Z_{j\tau}}\ln\langle\Phi(Z)|\Phi(Z)\rangle, \tag{5}$$

where $\sigma,\tau=x,y,z$ and $\mathcal{H}$ is the expectation value of Hamiltonian H by the use of $|\Phi\rangle$. In this paper we adopted the Gogny force [13] as the effective central force in the Hamiltonian. The Gogny force contains a finite-range two-body force and a density-dependent zero-range repulsive force and it gives a momentum-dependent mean field. The binding energies of ^{4}He, ^{12}C, and ^{14}N are calculated to be 28.3 MeV, 92.1 MeV, and 108.3 MeV, respectively, which are very close to their observed values, 28.3 MeV, 92.2 MeV, and 104.7 MeV, respectively.

When we apply AMD to heavy ion reactions, nucleon-nucleon collision processes should be incorporated. In AMD, as in QMD, two nucleons scatter stochastically when the spatial distance between them is small. But because of the effect of antisymmetrization, the centers of the Gaussians Z do not always have meaning as the positions and momenta of

nucleons. So we have to transform the coordinates Z to the physical coordinates $W=\{\mathbf{W}_i\}$ which can be interpreted as the positions and momenta of nucleons,

$$\mathbf{W}_i=\sum_{j=1}^{A}(\sqrt{Q})_{ij}\mathbf{Z}_j, \tag{6}$$

where

$$Q_{ij}=\frac{\partial}{\partial(\mathbf{Z}_i^*\cdot\mathbf{Z}_j)}\ln\langle\Phi(Z)|\Phi(Z)\rangle. \tag{7}$$

The real part $\mathbf{R}_i$ and the imaginary part $\mathbf{P}_i$ of $\mathbf{W}_i$,

$$\mathbf{W}_i=\sqrt{\nu}\mathbf{R}_i+\frac{i}{2\hbar\sqrt{\nu}}\mathbf{P}_i, \tag{8}$$

can be treated as physical positions and momenta of nucleons, respectively, in two-nucleon collisions. So in AMD when the physical positions $\mathbf{R}_i$ and $\mathbf{R}_j$ of two nucleons become close, two-nucleon collisions can occur and $W=\{\mathbf{W}_i\}$ changes into $W'=\{\mathbf{W}'_i\}$. We have to calculate the time development of Z after two-nucleon collisions have occurred. So we must retransform W' into Z'. But it can happen that there do not exist the coordinates Z' corresponding to W'. If this situation occurs, this two-nucleon collision is not realized. We call those W' which have no corresponding Z' Pauli forbidden and others Pauli allowed. The above definition of the Pauli forbidden and allowed regions is the extension of that of the time-dependent cluster model [14]. This is the picture of the Pauli principle in AMD. In AMD the fermionic nature of nucleons is exactly treated, because the wave function of an A-body system is antisymmetrized by a Slater determinant. Hence the Pauli principle has been fully incorporated.

We use the in-medium nucleon-nucleon cross section $\sigma_{NN}=\min\{\sigma^f_{NN},\sigma^d_{NN}\}$, the same as in Ref. [15]. Here σ^f_{NN} are based on the data of free cross sections and are parametrized as

$$\sigma^f_{pn}=\max\{13335(E/\mathrm{MeV})^{-1.125},40\}\ \ \mathrm{mb}, \tag{9}$$

$$\sigma^f_{pp}=\sigma^f_{nn}=\max\{4445(E/\mathrm{MeV})^{-1.125},25\}\ \mathrm{mb}, \tag{10}$$

and σ^d_{NN} is the density-dependent cross section and is given as

$$\sigma^d_{pn}=\sigma^d_{pp}=\sigma^d_{nn}=\frac{100\ \ \mathrm{mb}}{1+E/(200\ \ \mathrm{MeV})+C\ \min\{(\rho/\rho_0)^{1/2},1\}} \tag{11}$$

where ρ_0 is the normal density and the parameter C controls the reduction of the cross section due to the medium effect and is taken here as $C=2$. The angular distribution of proton-proton and neutron-neutron collisions is assumed to be isotropic while that of proton-neutron collisions is taken as

$$\frac{d\sigma_{pn}}{d\Omega}\propto 10^{-\alpha(\pi/2-|\theta-\pi/2|)}, \tag{12}$$

$$\alpha=\frac{2}{\pi}\max\{0.333\ \ln[E/(1\ \ \mathrm{MeV})]-1,0\}. \tag{13}$$

We calculate the time development of the system with AMD until a certain time $t=t_{\mathrm{SW}}$ when produced fragments are thermally equilibrated. At this time many excited fragments exist, and these thermally equilibrated fragments evaporate particles or γ rays with a long time scale. We calculate the evaporation process after t_{SW} by a multistep statistical decay code [16] which is similar to the code of Pühlhofer [17]. In this paper we take t_{SW} 150 fm/c and, in the following, call the process before t_{SW} ''the dynamical process'' and the one after t_{SW} ''the statistical decay process.'' In this paper we simulate the reactions of $p+^{12}$C at 26, 55, and 100 MeV and $\alpha+^{12}$C at 22.5 and 35 MeV/nucleon, and ^{14}N$+^{12}$C at 35 and 55 MeV/nucleon and we calculate about 20 000 events in each reaction.

III. COMPARISON OF AMD RESULTS WITH EXPERIMENTAL DATA

In order to examine the reliability of AMD calculations, we compare AMD results for the production cross sections of fragments with the experimental data for $p+^{12}$C at 55 MeV [18], $\alpha+^{12}$C at 22.5 MeV/nucleon [19], and ^{14}N $+^{12}$C at 35 MeV/nucleon [20] in Fig. 2. The solid and dashed lines indicate the AMD results and the experimental data, respectively. The AMD calculations reproduce the experimental data well in the whole mass range, except for the production cross section of fragments with $A=7$, in all reactions.

IV. MASS DISTRIBUTIONS

In this section, by comparing mass distributions from ^{12}C fragmentation at different incident energies and/or for different projectiles, we investigate how the excitation of alpha-cluster degrees of freedom depends on the incident energy and/or projectile.

Figure 3 shows mass distributions from ^{12}C fragmentation in ^{14}N induced reactions at 35 and 55 MeV/nucleon. As shown in the right panel, intermediate-mass fragments are slightly more produced and nucleons are more emitted at 55 MeV/nucleon than at 35 MeV/nucleon after statistical decay. This abundance of intermediate-mass fragments and nucleons at higher incident energy is a natural result due to the larger input energy to the system. However, as far as ^{4}He fragments are concerned, one finds that the production cross section at 35 MeV/nucleon is larger than that at 55 MeV/nucleon. This abundance of ^{4}He fragments at lower incident energy cannot be explained by the above conjecture. As shown in the left panel, the feature mentioned above becomes clearer before statistical decay. Especially, ^{4}He fragments are much more produced by the dynamical process at 35 MeV/nucleon than at 55 MeV/nucleon and, moreover, the production cross section of fragments with $A=8$, which are almost ^{8}Be fragments, runs out in neighboring mass fragments at 35 MeV/nucleon and this phenomenon is not seen at 55 MeV/nucleon. Accordingly, it is expected that alpha-cluster degrees of freedom in the ^{12}C nucleus are more easily excited at lower incident energy during the dynamical pro-

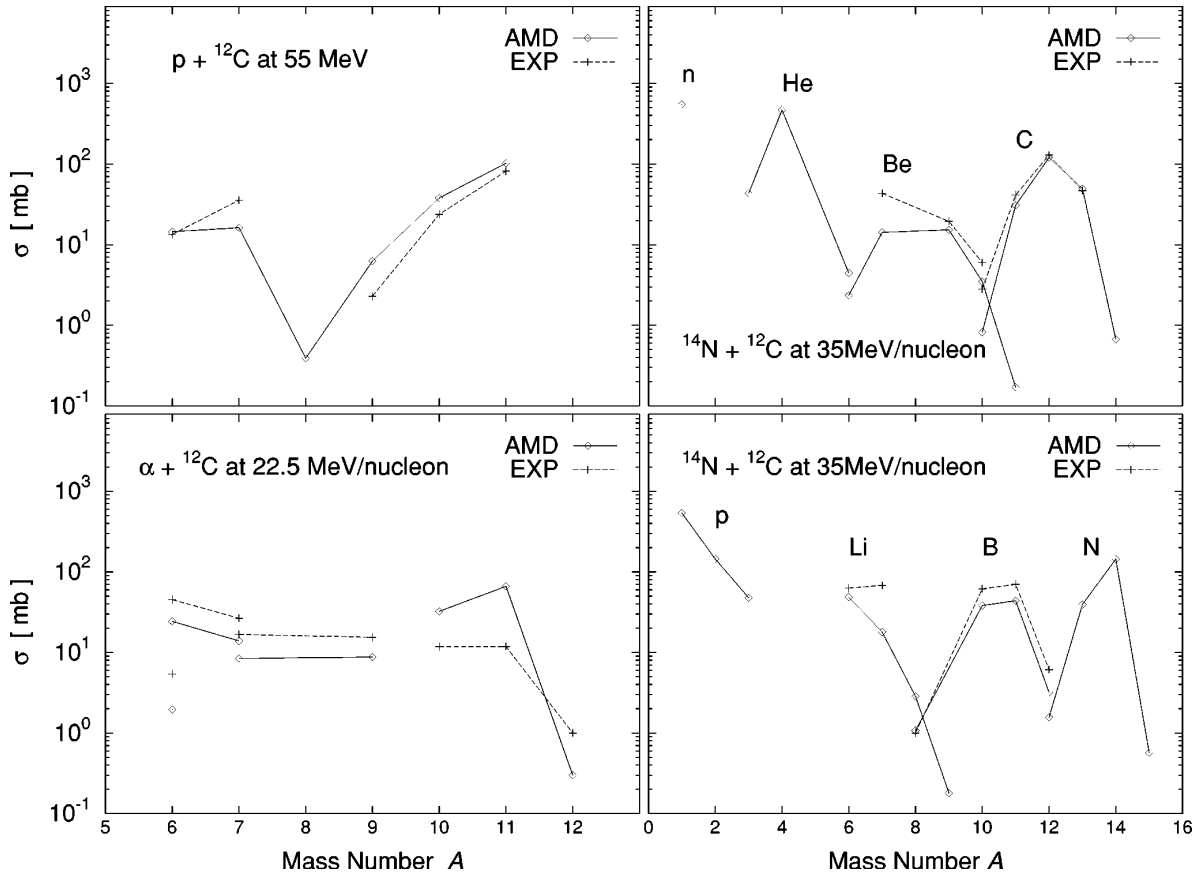

FIG. 2. Mass distribution in the $p+{}^{12}\mathrm{C}$ reaction at 55 MeV, isotope distributions in the $\alpha+{}^{12}\mathrm{C}$ at 22.5 MeV/nucleon, and those in the ${}^{14}\mathrm{N}+{}^{12}\mathrm{C}$ reactions at 35 MeV/nucleon. Solid lines indicate the AMD calculations and dashed lines indicate the experimental data.

cess in the ^{14}N induced reaction.

Figure 4 shows mass distributions in alpha induced reactions at 22.5 and 35 MeV/nucleon. As common as in ^{14}N induced reactions, slightly fewer intermediate-mass fragments are produced and more ^{4}He fragments are produced after statistical decay in the lower incident-energy reaction and this difference is more pronounced before statistical decay. Furthermore, the production cross section of fragments with $A=8$ also runs out in neighboring mass fragments before statistical decay. From the above results, we get the same conclusion as in the case of ^{14}N-projectile reactions; namely, we conclude that also in the α induced reaction alpha-cluster degrees of freedom in the ^{12}C nucleus are more easily excited during the dynamical process and ^{4}He fragments become abundant at lower incident energy. Another distinct difference between the two incident energies in alpha induced reactions is that the production cross sections of fragments above $A=12$ at 22.5 MeV/nucleon are much larger than those at 35 MeV/nucleon. This is not clearly seen in ^{14}N induced reactions. Since the lower incident energy in

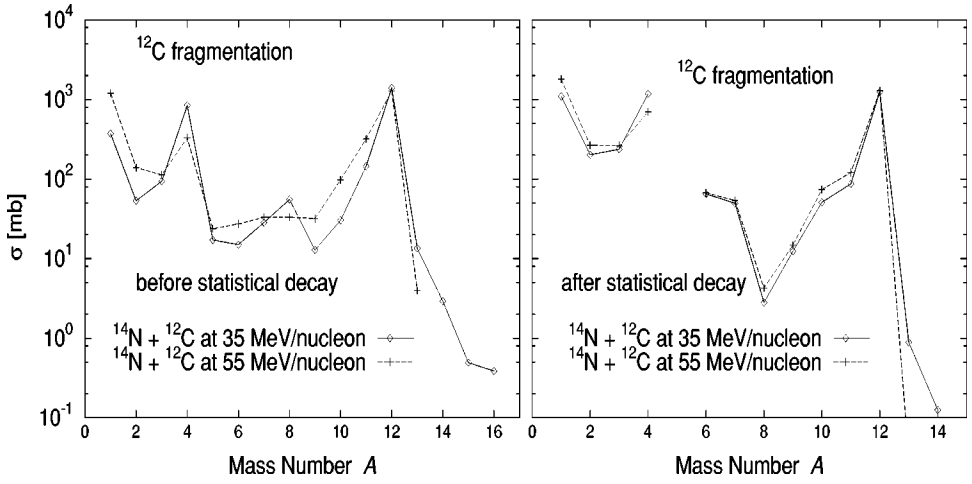

FIG. 3. Mass distributions from ^{12}C fragmentation in $^{14}\mathrm{N}+{}^{12}\mathrm{C}$ at 35 MeV/nucleon (solid lines) and 55 MeV/nucleon (dashed lines). Left and right panels show those before and after statistical decay, respectively.

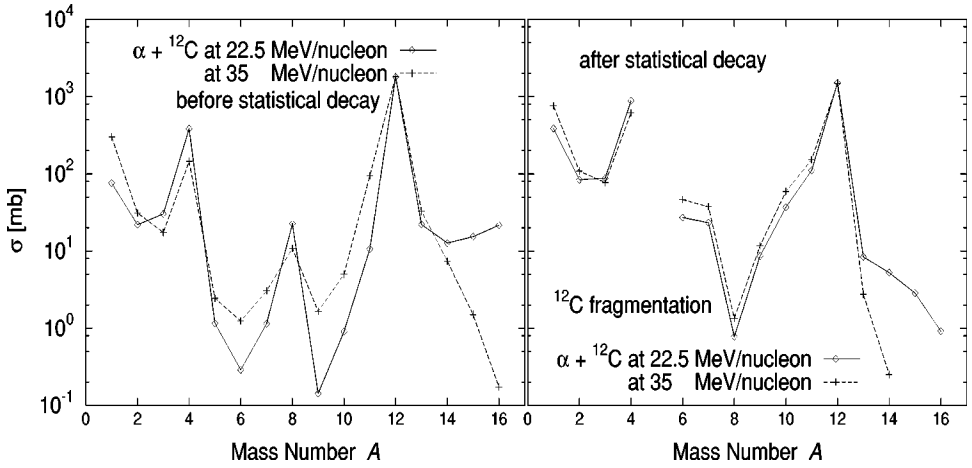

FIG. 4. Mass distributions in α induced reactions at 22.5 MeV/nucleon (solid line) and 35 MeV/nucleon (dashed line). Left panel and right panels indicate those before and after statistical decay, respectively.

^{14}N induced reactions is 35 MeV/nucleon, and is larger than the lower incident energy, 22.5 MeV/nucleon, in alpha induced reactions, it is natural that the transfer reaction more easily occurs at lower incident energy, namely, smaller relative velocity.

Mass distributions in proton induced reactions at 26 MeV, 55 MeV, and 100 MeV are shown in Fig. 5. As shown in the right panel, one finds that the mass distribution after statistical decay at 26 MeV is quite different from those at 55 and 100 MeV which are almost the same as each other. At the lowest incident energy fewer intermediate-mass fragments are produced; namely, ^{12}C fragmentation hardly occurs at 26 MeV compared with the reactions at the other two incident energies. However, the production cross section of ^{4}He fragments at 26 MeV is larger than those at 55 and 100 MeV. One might think that alpha-cluster degrees of freedom are more easily excited during the dynamical process at lower incident energy as in the case of α and ^{14}N induced reactions but this is not true. As shown in the left panel, not only the production cross section of intermediate-mass fragments but also that of ^{4}He fragments before statistical decay becomes smaller with decreasing incident energy. This indicates that the abundance of ^{4}He fragments after statistical decay at lower incident energy does not result from the dynamical process but from the statistical decay process, which is different from the result obtained in alpha and ^{14}N induced reactions where the abundance of ^{4}He fragments in ^{12}C fragmentation at lower incident energy results from the dynamical process.

V. EXCITATION ENERGIES OF ^{12}C DURING THE DYNAMICAL PROCESS

In the previous section, it is made clear that more ^{4}He fragments are produced at lower incident energies in all three kinds of projectile reactions, but its mechanism in proton induced reactions is different from that in alpha and ^{14}N induced reactions. The abundance of ^{4}He fragments at lower incident energy in alpha and ^{14}N induced reactions mainly results from the dynamical process; on the other hand, that in proton induced reactions mainly results from the statistical decay process. In this section we present definite evidence that alpha-cluster degrees of freedom are excited during the dynamical process in alpha and ^{14}N induced reactions by

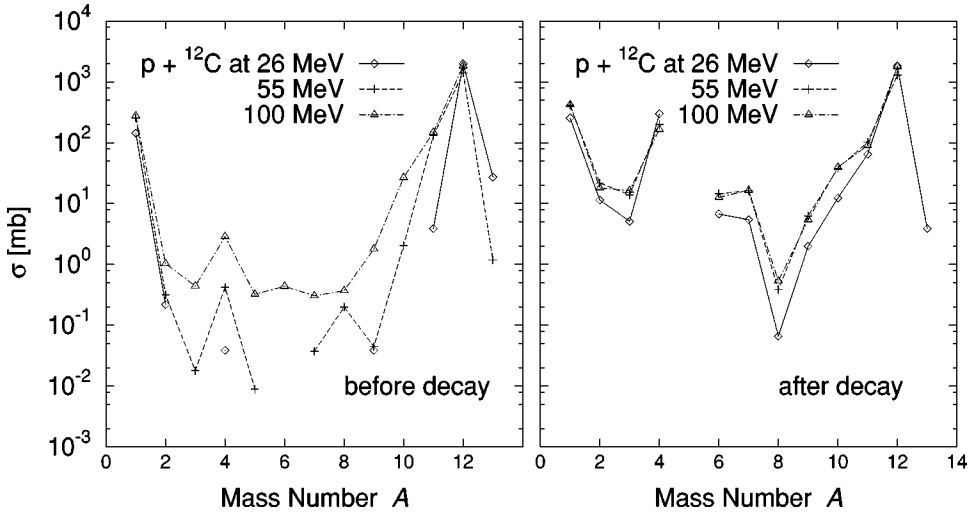

FIG. 5. Mass distributions in proton induced reactions at 26 MeV (solid line), 55 MeV (dashed line), and 100 MeV (dot-dashed line). Left and right panels indicate those before and after statistical decay, respectively.

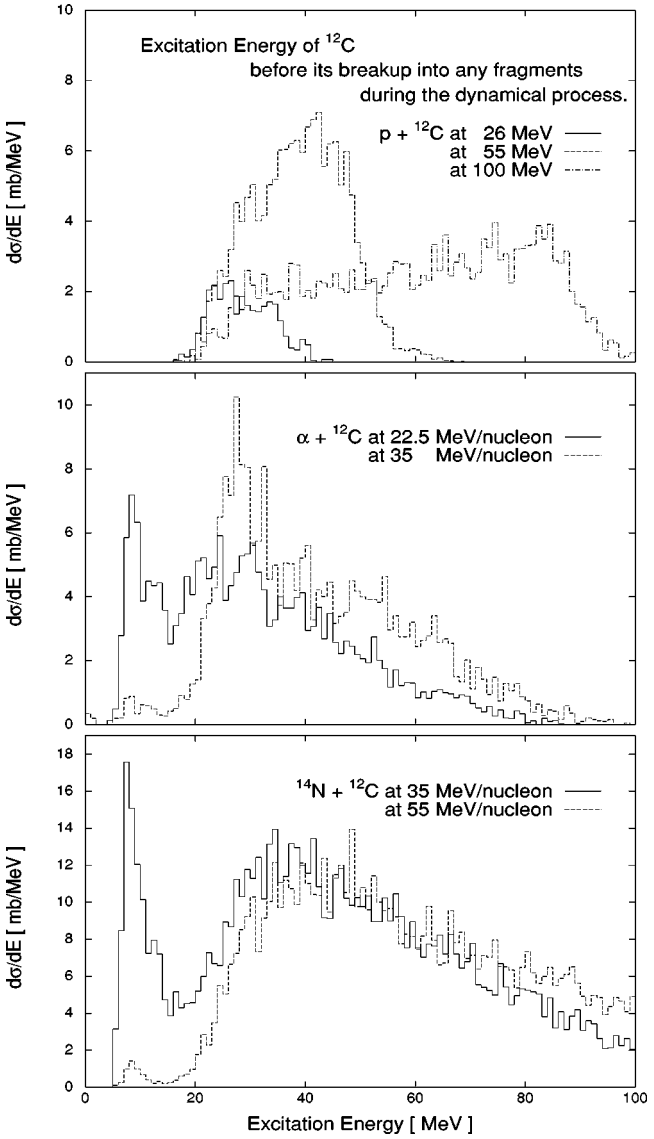

FIG. 6. Excitation energy spectra of ^{12}C just before its breakup into any fragments during the dynamical process. Upper panel shows those in the proton induced reaction at 26 MeV (solid line), 55 MeV (dashed line), and 100 MeV (dot-dashed line). Middle panel shows those in the alpha induced reaction at 22.5 MeV/nucleon (solid line) and 35 MeV/nucleon (dashed line). Lower panel shows those in the ^{14}N induced reaction at 35 MeV/nucleon (solid line) and 55 MeV/nucleon (dashed line).

showing the excitation energy spectra of ^{12}C just before its breakup into any fragments during the dynamical process.

The excitation energy of the isolated ^{12}C is calculated at each time step in the AMD simulations from the centers of Gaussians $\{\mathbf{Z}\}$ which originally constituted the initial ground state of ^{12}C and Fig. 6 displays the excitation energies of ^{12}C just before its breakup into any fragments during the dynamical stage in proton, α, and ^{14}N induced reactions. As seen clearly, the proton induced reaction is quite different from the other two kinds of projectile reactions. In α and ^{14}N induced reactions at lower incident energies the excitation energy spectra of ^{12}C just before its breakup into any fragments during the dynamical stage have two components; namely, one distributes in the region of 7–15 MeV and the other distributes in the region above 15 MeV. On the other hand, those in proton induced reactions have only the latter component even at lower incident energy. Since the former component just corresponds to the energy region of the excited levels of ^{12}C which have the 3α cluster structure, it is expected that alpha-cluster degrees of freedom are excited in α- and ^{14}N-projectile reactions at lower incident energy during the dynamical process. On the other hand, in proton induced reactions, even at the lowest incident energy, it is hard for alpha-cluster states to be excited during the dynamical process and it is expected that shell-model-like excited states are mainly excited since the rising point of the latter component roughly corresponds to the threshold of one-nucleon emission from ^{12}C nucleus.

This former component, which is related to the excitation of alpha-cluster degrees of freedom, disappears at higher incident energies in alpha and ^{14}N induced reactions. This suggests that there is a border where alpha-cluster degrees of freedom are excited or not and this boundary incident energy is dependent on projectiles. In the alpha induced reaction the boundary incident energy exists between 22.5 MeV/nucleon and 35 MeV/nucleon, while in the ^{14}N induced reaction it exists between 35 MeV/nucleon and 55 MeV/nucleon.

VI. MEAN-FIELD EFFECT ON THE EXCITATION OF ALPHA-CLUSTER DEGREES OF FREEDOM

We consider that the excitation of alpha-cluster degrees of freedom is caused by the mean-field effect from the projectile. Namely, we consider that the mean field from the projectile excites ^{12}C to the states which have the alpha-cluster structure. On the other hand, nucleon-nucleon collision processes destroy the activation of the alpha clustering in the ^{12}C nucleus. We can examine this conjecture within the AMD framework by switching off nucleon-nucleon collision processes.

Figure 7 displays the excitation energy spectra of ^{12}C just before its breakup into any fragments during the dynamical process with and without nucleon-nucleon collision processes, which are indicated by solid and dashed lines, respectively. The upper and lower panels show those in ^{14}N induced reactions at 35 and 55 MeV/nucleon, respectively. By comparing the solid and dashed lines, we can say that the excitation of ^{12}C to the states whose excitation energies are 7–15 MeV is caused by the mean field from the projectile while nucleon-nucleon collision processes reduce this excitation. It should be noted that the mean field excites alpha-cluster degrees of freedom not only at 35 MeV/nucleon but also at 55 MeV/nucleon. However, the peak height without nucleon-nucleon collisions at 35 MeV/nucleon is higher than that at 55 MeV/nucleon. This can be interpreted in terms of the interaction time. At 35 MeV/nucleon ^{14}N has a slower relative velocity compared with the case at 55 MeV/nucleon, and so the ^{12}C nucleus can ''feel'' the mean field from the ^{14}N nucleus for a longer time. As a result, the mean-field effect at 35 MeV/nucleon becomes larger than that at 55 MeV/nucleon.

With inclusion of nucleon-nucleon collisions, the excitation of ^{12}C to the excitation energy region 7–15 MeV is largely reduced. At 35 MeV/nucleon the component from 7 to 15 MeV survives due to the large effect of the mean field; on the other hand, at 55 MeV/nucleon this component disap-

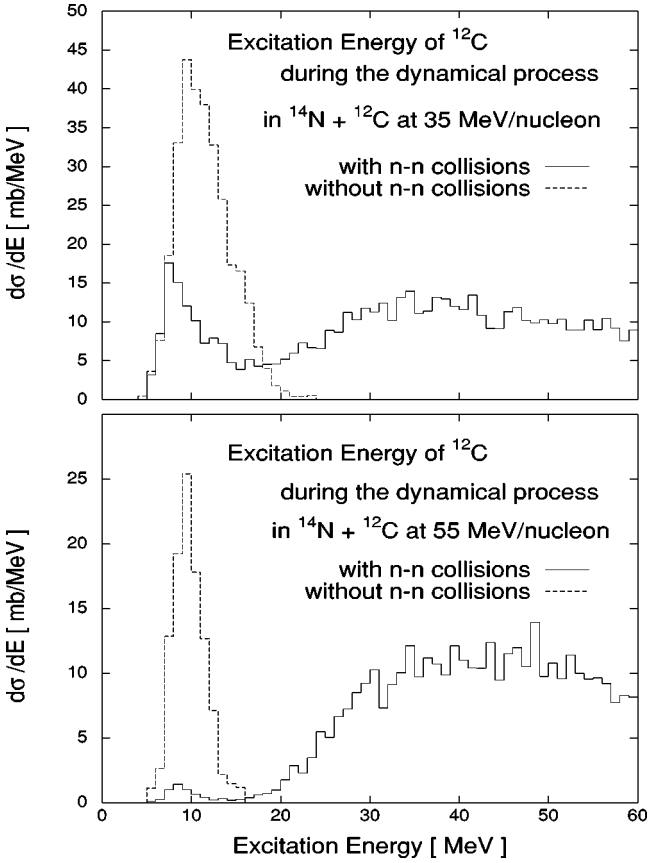

FIG. 7. Excitation energy spectra of ^{12}C just before its breakup into any fragments during the dynamical process. Upper and lower panels show those in ^{14}N induced reactions at 35 and 55 MeV/nucleon, respectively. Solid and dashed lines indicate those with and without nucleon-nucleon collision processes, respectively.

pears due to the weaker effect of the mean field and the stronger effect of nucleon-nucleon collision processes.

Furthermore, one can see that the component above 15 MeV is generated by nucleon-nucleon collision processes. In the previous section we have shown that the boundary incident energy where alpha-cluster degrees of freedom are excited or not depends on the projectile. This dependence of the boundary incident energy is interpreted in the term of the mean-field effect. Since the ^{14}N nucleus has a larger mean-field effect than the α particle, the ^{14}N projectile can excite alpha-cluster degrees of freedom in the ^{12}C nucleus even for a shorter interaction time compared with the α projectile. As a result, the boundary incident energy in the ^{14}N-projectile reaction is higher than that in the α-projectile reaction.

VII. ^{4}He-MULTIPLICITY CHANNELS

In our previous paper [12] we indicated that the abundance of ^{4}He fragments from ^{12}C fragmentation compared with ^{14}N fragmentation mainly results from the process of $^{12}\mathrm{C}\rightarrow 3\alpha$ during the dynamical process. In this section we analyze the production of ^{4}He fragments in terms of ^{4}He-multiplicity channels.

Table I shows multiplicity-channel cross sections of ^{4}He fragments classified by the multiplicity of ^{4}He fragments before and after statistical decay in the ^{14}N induced reaction at 35 MeV/nucleon and 55 MeV/nucleon. The gains of the cross sections after statistical decay compared with the ones before statistical decay are also given. The total production cross sections of ^{4}He fragments are also listed in the last line, which are obtained from the sum of multiplicity-channel cross sections multiplied by their multiplicity of ^{4}He fragments. The difference of the total production cross section of ^{4}He fragments before statistical decay between two incident energies is about 580 mb and that after statistical decay is about 490 mb. From this, we see that the abundance of ^{4}He fragments at 35 MeV/nucleon mainly results from the dynamical process, which is consistent with the results obtained previously. By comparing multiplicity-channel cross sections between two incident energies, we find that the channel cross section of multiplicity 3 events at 55 MeV/nucleon is extremely small while the multiplicity 3 channel makes a significant contribution to the abundance of ^{4}He fragments at lower incident energy in the ^{14}N induced reaction. Moreover, from the gain of the multiplicity 3 channel, we see that the statistical component of the multiplicity 3 events plays a minor role in the production of ^{4}He fragments and its amount is almost the same at both incident energies. This means that the abundance of ^{4}He fragments at lower incident energy is caused by the multiplicity 3 events during the dynamical process, which is consistent with the result obtained in the previous paper [12].

Table II shows multiplicity-channel cross sections in alpha induced reactions at 22.5 and 35 MeV/nucleon in the same manner as in Table I. With respect to the total production cross section of ^{4}He fragments the difference between two incident energies before statistical decay is about 250 mb and that after statistical decay becomes about 280 mb.

TABLE I. Multiplicity-channel cross sections (in units of mb) classified by the multiplicity of ^{4}He fragments in ^{14}N induced reactions at 35 MeV/nucleon and 55 MeV/nucleon. Those before and after statistical decay are listed, together with the gains of cross sections after statistical decay compared to the ones before statistical decay. The total production cross sections of ^{4}He fragments are also shown in the last line.

^{4}He-multiplicity	^{14}N+^{12}C at 35 MeV/nucleon			^{14}N+^{12}C at 55 MeV/nucleon		
channel	Before decay	After decay	Gain	Before decay	After decay	Gain
1	120.7	152.4	31.7	82.9	173.3	90.4
2	98.5	200.5	102.0	63.8	184.0	120.2
3	175.2	207.2	32.0	17.0	49.2	32.2
Cross section	843	1175	332	261	689	428

TABLE II. Multiplicity-channel cross sections (in units of mb) of each ^{4}He multiplicity events in alpha induced reactions at 22.5 MeV/nucleon and 35 MeV/nucleon. The total production cross section of ^{4}He fragments is shown in the last line.

^{4}He-multiplicity channel	$\alpha+^{12}$C at 22.5 MeV/nucleon			$\alpha+^{12}$C at 35 MeV/nucleon		
	Before decay	After decay	Gain	Before decay	After decay	Gain
1	17.5	49.7	32.2	20.8	61.5	40.7
2	13.5	48.5	35.0	7.66	85.6	77.9
3	80.4	216.3	135.9	30.7	125.3	94.6
4	24.5	21.9	−2.6	1.02	0.13	−0.89
Cross section	384	883	499	132	609	477

Since the difference between the total production cross section before and after statistical decay is almost the same and the gains from the statistical decay process are also similar to each other, the abundance of ^{4}He fragments at lower incident energy in the alpha induced reaction mainly results from the dynamical process, which is the same result as in the ^{14}N-projectile reaction. Moreover, before statistical decay, the channel cross sections of multiplicity 1 and 2 events in the reaction at 22.5 MeV/nucleon are comparable to those in the reaction at 35 MeV/nucleon but the channel cross section of multiplicity 3 events at 22.5 MeV/nucleon is much larger than that at 35 MeV/nucleon. So we see clearly that these multiplicity 3 events during the dynamical process causes an abundance of ^{4}He fragments at lower incident energy in the alpha induced reaction. As far as the statistical decay process is concerned, in the reaction at 22.5 MeV/nucleon, the multiplicity 3 events are still important because their gain from the statistical decay process is much larger compared to that of other multiplicity events. This is a very different feature from the case in ^{14}N induced reactions. The reason for this fact will be given in terms of excitation energies of ^{12}C at the end of the dynamical process in Sec. VIII. In addition, there is a certain amount of multiplicity 4 events in the alpha induced reaction at 22.5 MeV/nucleon. This suggests that the production mechanism of ^{4}He fragments via the compound nucleus, which is formed by the capture of the incident alpha particle by the ^{12}C nucleus, appears at lower incident energy and this process becomes non-negligible. Note that we here only count alpha particles scattered backward in the nucleon-nucleon center-of-mass system.

Table III lists multiplicity-channel cross sections of ^{4}He fragments and the total production cross sections of ^{4}He fragments in proton induced reactions at 26, 55, and 100 MeV, in the same manner as in Tables I and II, but only cross sections after statistical decay are listed because ^{4}He fragments are scarcely produced before statistical decay, as indicated in Fig. 5. The production cross sections of ^{4}He fragments become smaller with increasing incident energy, but we should recall that the source of the abundance of ^{4}He fragments at 26 MeV is due to the statistical decay process, which is different from the case in α and ^{14}N induced reactions. It is clearly seen in Table III that the abundance of ^{4}He fragments at the lowest incident energy results from the multiplicity 3 channel. The channel cross section of multiplicity 3 events after statistical decay becomes larger as the incident energy decreases and the channel cross sections of multiplicity 1 and 2 events become negligible at 26 MeV. This suggests that the breakup of the ^{12}C nucleus into 3α particles by the statistical decay process becomes important for ^{4}He production at the lowest incident energy. On the other hand, the cross sections of multiplicity 1 and 2 events become large at high incident energies. This result is regarded as being natural in the following way. At higher incident-energy collisions ^{12}C nuclei more easily break up during the dynamical process, and if the ^{12}C nucleus emits only a nucleon before statistical decay, it cannot break up into 3α particles any longer by the statistical decay process. So the contribution of equilibrated fragments at the end of the dynamical process becomes important for the production of ^{4}He fragments in the proton induced reaction at high incident energies. Furthermore, as will be shown in Fig. 8, there exist highly excited ^{12}C nuclei at the end of the dynamical process and these nuclei are expected to make a contribution to the multiplicity 1 and 2 channels at high incident energies.

TABLE III. Cross sections (in units of mb) of each ^{4}He multiplicity events after statistical decay in proton induced reactions at 26 MeV, 55 MeV, and 100 MeV.

Multiplicity of ^{4}He fragments	$p+^{12}$C at 26 MeV	at 55 MeV	at 100 MeV
1	7.6	25.1	23.5
2	6.8	28.2	38.8
3	92.3	39.4	21.5
Cross section	298	200	166

VIII. EXCITATION OF COMPOUND STATES OF ^{12}C

The excitation energy spectra of ^{12}C at the end of the dynamical process, namely, at $t=t_{\mathrm{SW}}$, are shown in Fig. 8. The left panel shows those in proton induced reactions and the solid, dashed, and dot-dashed lines indicate those at 26 MeV, 55 MeV, and 100 MeV, respectively. One finds immediately that there are two distinct features. The first one is that more ^{12}C nuclei are excited in the region of 5–20 MeV with decreasing incident energy. These low excited ^{12}C nuclei are expected to break up into 3α particles, and as a result, the channel cross section of multiplicity 3 events becomes larger with decreasing incident energy, as is shown in Table III, and this sequential statistical decay process of $^{12}\mathrm{C}\rightarrow 3\alpha$ increases the abundance of ^{4}He fragments in the lowest incident-energy reaction compared with higher

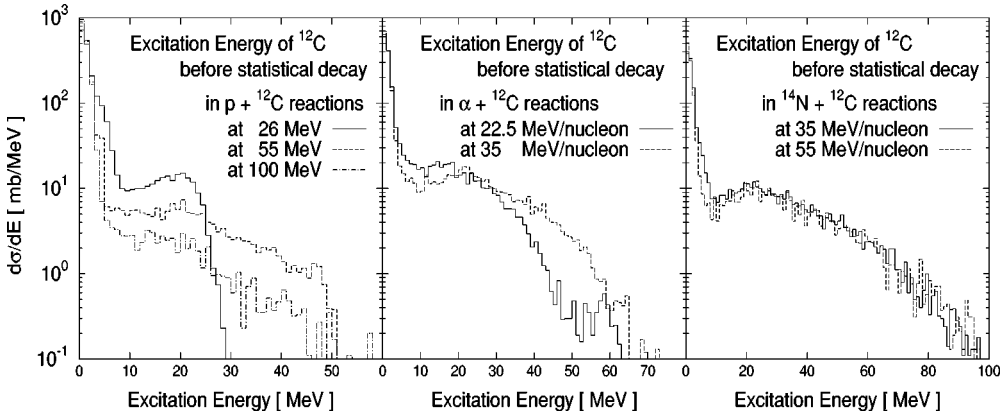

FIG. 8. Excitation energy spectra of ^{12}C at the end of the dynamical process. Left panel shows those in proton induced reactions at 26 (solid line), 55 (dashed line), and 100 MeV (dot-dashed line). Middle panel shows those in alpha induced reactions at 22.5 MeV/nucleon (solid line) and 35 MeV/nucleon (dashed line). Right panel shows those in ^{14}N induced reactions at 35 MeV/nucleon (solid line) and 55 MeV/nucleon (dashed line).

incident-energy reactions. The second feature appears in the high excitation energy region. Because of the small input energy into the system, the ^{12}C nucleus is not so highly excited in the reaction at 26 MeV. In contrast, the ^{12}C nucleus is excited up to about 50 MeV in the reactions at 55 and 100 MeV and saturation of the excitation energies of ^{12}C nuclei is seen. In the reaction at 100 MeV it is possible for the ^{12}C nucleus to be excited in the region above 50 MeV, but the excitation energy spectrum at 100 MeV incident energy distributes only below 50 MeV. This, we think, is an important reason why the mass distributions at 55 MeV and 100 MeV are similar to each other after statistical decay, as was indicated by the right panel in Fig. 5. This kind of saturation of the excitation energy is also seen in alpha and ^{14}N induced reactions, as is shown in the middle and right panels. The saturation energies in proton-, alpha-, and ^{14}N-projectile reactions are 50, 65, and 95 MeV, respectively. From these results, we suggest that saturation of the excitation energy of the ^{12}C nucleus depends on the projectile, and the larger the projectile mass is, the higher the saturation energy of ^{12}C becomes.

In the middle panel, we show the excitation energy spectra of ^{12}C at the end of the dynamical process ($t=t_{\mathrm{SW}}$) in alpha induced reactions at 22.5 (solid line) and at 35 MeV/nucleon (dashed line). The same features as in the case of proton induced reactions are clearly seen. Excited ^{12}C nuclei at the end of the dynamical process in the collisions at 22.5 MeV/nucleon are more populated in the region from about 5 MeV to 20 MeV than in the collisions at 35 MeV/nucleon. Reflecting this result, the statistical decay process of the multiplicity 3 events makes a relatively large contribution to the production of ^{4}He fragments in the alpha induced reaction at 22.5 MeV/nucleon, as is shown in Table II. Moreover, more highly excited ^{12}C nuclei are produced at 35 MeV/nucleon compared with the case at 22.5 MeV/nucleon. This is one of the reasons why the statistical components of the multiplicity 2 events have a larger contribution in the higher incident-energy reaction. In addition, as is shown in Fig. 4, more intermediate-mass fragments with $A=9-11$ are produced during the dynamical process at higher incident energy, and these fragments reduce the larger contribution of the multiplicity 2 events by the statistical decay process in the higher incident-energy reaction.

The right panel shows excitation energy spectra of ^{12}C at the end of the dynamical process ($t=t_{\mathrm{SW}}$) in ^{14}N induced reactions at 35 MeV/nucleon (solid line) and at 55 MeV/nucleon (dashed line). Excited ^{12}C nuclei at the end of the dynamical process at both incident energies are almost the same as each other. By reflecting this similarity, the channel cross sections of the multiplicity 3 events from the statistical decay process have almost the same value in the ^{14}N induced reaction at both incident energies, as is shown in Table I, and the lack of excited ^{12}C in the region of 5–20 MeV reduces the statistical component of multiplicity 3 channel. But we cannot conclude that the multiplicity 3 events from the statistical decay process are always minor contributions in ^{14}N induced reactions without further investigation of the lower incident-energy reactions. In spite of this similarity the multiplicity 1 and 2 events due to the statistical decay process are more frequent at 55 MeV/nucleon than those at 35 MeV/nucleon, as shown in Table I. This is caused by the intermediate-mass fragments produced during the dynamical process, more of which are produced at 55 MeV/nucleon than those at 35 MeV/nucleon.

IX. SUMMARY AND CONCLUSION

We have analyzed ^{12}C fragmentation in proton, alpha, and ^{14}N induced reactions at two or three incident energies using the AMD method. More ^{4}He fragments are produced at lower incident energy in all three kinds of projectile reactions. But the source of the abundance of ^{4}He fragments at lower incident energy is different among the three projectile reactions. In alpha and ^{14}N induced reactions this mainly results from the dynamical process, while in proton induced reactions this mainly results from the statistical decay process. In alpha and ^{14}N induced reactions at lower incident energy, the excitation energy spectra of ^{12}C just before its breakup into any fragments during the dynamical process have a component whose peak is located around 10 MeV and this component disappears at higher incident energy. Since this energy region corresponds to the excited levels of ^{12}C

which are recognized to have the 3α cluster structure, it is expected that the alpha-cluster degrees of freedom are excited during the dynamical process in the lower incident-energy reaction. On the other hand, in proton induced reactions this component of the excitation energy spectra is not seen at all incident energies. This suggests that it is hard for alpha-cluster degrees of freedom to be excited during the dynamical process in the proton induced reaction even at lower incident energy. Accordingly we conclude that the excitation of alpha-cluster degrees of freedom during the dynamical process depends on the incident energy and/or the projectile.

Furthermore, the boundary of the incident energy whether alpha-cluster degrees of freedom are excited or not during the dynamical process is different between alpha- and ^{14}N-projectile reactions. The boundary incident energies in alpha and ^{14}N induced reactions are around 30 MeV/nucleon and 40 MeV/nucleon, respectively. This shows that the boundary incident energy is also dependent on the projectile.

We have investigated the character of the excitation of alpha-cluster degrees of freedom during the dynamical process which results from the mean-field effect. We have done this investigation by switching off the nucleon-nucleon collision processes within the framework of the AMD method. When the nucleon-nucleon collision processes are switched off, the excitation energy spectra of ^{12}C have proved to have only one component which covers the excitation energy region of 7–20 MeV with a peak around 10 MeV in ^{14}N induced reactions at both incident energies. This suggests that alpha-cluster degrees of freedom are excited due to the mean-field effect. Furthermore, the peak height of the excitation energy spectrum of ^{12}C without nucleon-nucleon collisions becomes smaller for higher incident energy. The reduction of the peak height for higher incident energy can be interpreted to be due to the weakened effect of the projectile mean field for the shorter interaction time. We can conclude that the mean field of the projectile causes the excitation of ^{12}C to its clustering excited states while the two-nucleon collision process works to destroy this excitation and that the disappearance of the excitation to the clustering states at high incident energies is partly due to the weakened effect of the projectile mean field and partly due to the strengthened effect of the two-nucleon collision process.

As the mass of the projectile becomes larger, the mean-field effect becomes larger and it is easy for alpha-cluster degrees of freedom to be excited during the dynamical process. In proton-projectile reactions the proton gives so small a mean-field effect to the ^{12}C nucleus that alpha-cluster degrees of freedom are hard to be excited during the dynamical process. The dependence of the boundary incident energy on the projectile is also interpreted in terms of the mean-field effect. Since the ^{14}N nucleus has a larger mean-field effect on the ^{12}C nucleus compared with the alpha particle, the mean field from the ^{14}N nucleus can excite alpha-cluster degrees of freedom within a shorter interaction time compared with the α-projectile case; namely, the ^{14}N projectile can excite alpha-cluster degrees of freedom with a higher relative velocity compared with the α projectile. Accordingly, the boundary incident energy in the ^{14}N-projectile reaction is higher than that in the alpha-projectile reaction. Consequently there is a possibility that alpha-cluster degrees of freedom are excited during the dynamical process even in the proton-projectile reaction if the incident energy is much lower than the lower incident energy analyzed here. As the incident energy decreases, the wavelength of the incident proton becomes larger, but since the state of the incident proton is described by a Gauss packet with a fixed width in AMD, this effect is not included in the calculations here. It is a future problem whether the proton with lower incident energy cannot really excite alpha-cluster degrees of freedom during the dynamical process.

Most of the calculations for this research project were performed with the Fujitsu VPP500 of RIKEN, Japan.

[1] Proceedings of Fifth International Conference on Nucleus-Nucleus Collisions, Taormina, 1994, edited by M. Di Toro, E. Migneco, and P. Piatteli [Nucl. Phys. **A583**, 297 (1995)].

[2] K. Ikeda, H. Horiuchi, S. Saito, Y. Fujiwara, M. Kamimura, K. Kato, Y. Suzuki, E. Uegaki, H. Furutani, H. Kanada, T. Kaneko, S. Nagata, H. Nishioka, S. Okabe, T. Sakuda, M. Seya, Y. Abe, Y. Kondo, T. Matsuse, and A. Tohsaki-Suzuki, Prog. Theor. Phys. Suppl. **68**, 1 (1980).

[3] G. F. Bertsch and S. Das Gupta, Phys. Rep. **160**, 189 (1988).

[4] J. Aichelin and H. Stöcker, Phys. Lett. B **176**, 14 (1986); J. Aichelin, Phys. Rep. **202**, 233 (1991).

[5] A. Ono, H. Horiuchi, Toshiki Maruyama, and A. Ohnishi, Prog. Theor. Phys. **87**, 1185 (1992).

[6] A. Ono, H. Horiuchi, and Toshiki Maruyama, Phys. Rev. C **48**, 2946 (1993); A. Ono and H. Horiuchi, *ibid.* **51**, 299 (1995).

[7] E. I. Tanaka, A. Ono, H. Horiuchi, Tomoyuki Maruyama, and A. Engel, Phys. Rev. C **52**, 316 (1995); A. Engel, E. I. Tanaka, Tomoyuki Maruyama, A. Ono, and H. Horiuchi, *ibid.* **52**, 3231 (1995).

[8] R. J. Charity, J. Barreto, L. G. Sobotka, D. G. Sarantites, D. W. Stracener, A. Chbihi, N. G. Nicolis, R. Auble, C. Baktash, J. R. Beene, F. Bertrand, M. Halbert, D. C. Hensley, D. J. Horen, C. Ludemann, M. Thoennessen, and R. Varner, Phys. Rev. C **46**, 1951 (1992).

[9] B. A. Harmon, J. Pouliot, J. A. López, J. Suro, R. Knop, Y. Chan, D. E. Digregorio, and R. G. Stokstad, Phys. Lett. B **235**, 234 (1990).

[10] R. J. Charity, L. G. Sobotka, N. J. Robertson, D. G. Sarantites, J. Dinius, C. K. Gelbke, T. Glasmacher, D. O. Handzy, W. C. Hsi, M. J. Huang, W. G. Lynch, C. P. Montoya, G. F. Peaslee, C. Schwarz, and M. B. Tsang, Phys. Rev. C **52**, 3126 (1995).

[11] M. Samri, L. Beaulieu, B. Djerroud, D. Doré, R. Laforest, Y. Lacochelle, J. Pouliot, R. Roy, C. St-Pierre, G. C. Ball, A. Galindo-Uribarri, E. Hagberg, and D. Horn, Nucl. Phys. **A609**, 108 (1996).

[12] H. Takemoto, H. Horiuchi, A. Engel, and A. Ono, Phys. Rev. C **54**, 266 (1996).

[13] J. Dechargé and D. Gogny, Phys. Rev. C **21**, 1568 (1980).

[14] M. Saraceno, P. Kramer, and F. Fernandez, Nucl. Phys. **A405**, 88 (1983).
[15] A. Ono, H. Horiuchi, and T. Maruyama, Phys. Rev. C **48**, 2946 (1993).
[16] Toshiki Maruyama, A. Ono, A. Ohnishi, and H. Horiuchi, Prog. Theor. Phys. **87**, 1367 (1992).
[17] F. Pühlhofer, Nucl. Phys. **A280**, 267 (1977).
[18] C. T. Roche, R. G. Clark, G. J. Mathews, and V. E. Viola, Jr., Phys. Rev. C **14**, 410 (1976).
[19] M. Jung, C. Jacquot, C. Baixeras-Aiguabelia, R. Schmitt, and H. Braun, Phys. Rev. C **1**, 435 (1970).
[20] A. Kiss, F. Dék, Z. Seres, G. Caskey, A. Galonsky, B. Remington, and L. Heilbronn, Nucl. Phys. **A499**, 131 (1989).